2009

EFFECTS OF CALCIUM CHANGES ON HYSTERESIS IN RESTITUTION OF ACTION POTENTIAL DURATION

Kathleen Marie Guzman
University of Kentucky, rgaur2@uky.edu

ABSTRACT OF THESIS

EFFECTS OF CALCIUM CHANGES ON HYSTERESIS IN RESTITUTION OF
ACTION POTENTIAL DURATION

Sudden cardiac death (SCD) is a leading cause of fatalities. Several methods have been developed to predict instability in myocytes which could lead to SCD. The focus of this study was on altering memory in myocytes, i.e. hysteresis in restitution of action potential duration (APD), by differing levels of calcium. Determination of alteration was implemented by using a diastolic interval (DI) control program that implements a sinusoidal change in DI. Plotting APD versus previous DI, i.e. restitution, produces a hysteresis loop. From these hysteresis loops, five parameters were used to determine measures of memory: area, thickness, overall tilt, max delay and min delay. Calcium levels were then altered with either verapamil or BAPTA-AM. Statistically significant effects were found for the verapamil study, but not for the BAPTA-AM study. Simulations were used to explain significant results. The verapamil findings support clinical studies that have shown verapamil to not have anti-arrhythmic effects. Theory predicts that a decrease in memory would decrease the stability of a system, and perhaps verapamil may not increase stability as hypothesized previously. The results of the BAPTA-AM study were inconclusive, and further investigation is needed before it can be determined that BAPTA-AM has no significant effect on memory.

KEYWORDS: Hysteresis in restitution, L-type calcium channel, free intracellular calcium, memory, stability

Kathleen Marie Guzman
06/03/2009

EFFECTS OF CALCIUM CHANGES ON HYSTERESIS IN RESTITUTION OF
ACTION POTENTIAL DURATION

By

Kathleen Marie Guzman

Dr. Abhijit Patwardhan
Director of Thesis

Dr. Abhijit Patwardhan
Director of Graduate Studies

06/03/2009

RULES FOR THE USE OF THESES

Unpublished theses submitted for the Master's degree and deposited in the University of Kentucky Library are as a rule open for inspection, but are to be used only with due regard to the rights of the authors. Bibliographical references may be noted, but quotations or summaries of parts may be published only with the permission of the author, and with the usual scholarly acknowledgments.

Extensive copying or publication of the thesis in whole or in part also requires the consent of the Dean of the Graduate School of the University of Kentucky.

A library that borrows this thesis for use by its patrons is expected to secure the signature of each user.

Name   Date

_____

_____

_____

_____

_____

_____

_____

_____

_____

_____

THESIS

Kathleen Marie Guzman

The Graduate School

University of Kentucky

2009

EFFECTS OF CALCIUM CHANGES ON HYSTERESIS IN RESTITUTION OF
ACTION POTENTIAL DURATION

_____

THESIS

_____

A thesis submitted in partial fulfillment of the
requirements for the degree of Master of Science in
Biomedical Engineering in the Graduate School
at the University of Kentucky

By
Kathleen Marie Guzman
Lexington, Kentucky
Director: Dr. Abhijit Patwardhan, Professor of Biomedical Engineering
Lexington, Kentucky
2009

DEDICATION

I would like to dedicate this thesis to my mother for her endless support throughout my life. I would not be here without her helpful nudges in the right direction.

ACKNOWLEDGEMENTS

I would like to acknowledge my adviser, Dr. Abhijit Patwardhan, for his patience, extensive knowledge and guidance.

I would also like to acknowledge Anuj Agarwal for his help in experiments, and to Pooja Vijaygopal, Stuart Traxel and Anuj for being a valuable part of my work environment.

TABLE OF CONTENTS

LIST OF TABLES

LIST OF FIGURES

LIST OF FILES

Chapter One: Introduction

"Sudden cardiac death, a.k.a. sudden cardiac arrest, is a leading cause of death in the United States and has been for several decades. The mortality rate is over 600,000 per year in the US alone, and only half of the victims are hospitalized. The low percentage of hospitalization is due to the rapidity of sudden cardiac death. Partial death (brain death) as well as complete death can occur in four to six minutes, with chance of survival decreasing seven to ten percent every minute. This arrest of the heart is typically due to an irregular heart rhythm caused by an electrical abnormality such as bradycardia (subnormal heart rate), tachycardia (supernormal heart rate) or ventricular fibrillation (chaotic heart beat). This is not synonymous with the term heart attack, which refers to a lack of blood supply to the heart. However, a heart attack, along with all other heart diseases, could lead to sudden cardiac death. Sudden arrest can be stopped if treated immediately with either CPR or defibrillation."

The above information was paraphrased from the American Heart Association (AHA) website [1].

Due to the prominence and severity of this disease, the mechanisms of initiation and maintenance of ventricular fibrillation (VF) have been a main focus in research for decades. Walker and Rosenbaum have noted that alternans, or the alternation of electrophysiological properties from one beat to the subsequent beat, were seen before VF, which then lead to sudden cardiac death [2]. A heart beat consists of two phases: contraction, i.e. systole, and relaxation, i.e. diastole. In terms of electrical function of the heart, an action potential corresponds to systole; where as a diastolic interval (DI) corresponds to diastole. The electrophysiological relationship between systole and diastole has been functionally defined as the dependence of an APD on the previous DI. In the case of alternans, if a DI was shorter in length than its previous beat, the subsequent APD would be shorter causing a longer DI and thus a longer APD, and so on. The phenomenon of dependence of an APD on previous DI is widely known as electrical restitution, which is referred to as restitution in this document. This restitution should not

be confused with mechanical restitution [3] or the electrical restitution defined as the dependence of APD on a previous cycle length (CL) as seen in the past [4]. Nolasco and Dahlen noted that alternations in action potentials could occur with only one abrupt change in heart beat (i.e. experiencing an "unexpected" stimulus). Therefore, they sought to define the relationship between alternans and rate of pacing by creating a model that predicted the change in DIs and APDs seen by a change in CL, giving rise to the restitution curve. It was hypothesized that if a tangent to the slope of the restitution curve was one, steady state alternans occurred, if the slope was greater than one, unstable alternans occurred and if the slope was less than one, alternans did not exist [5]. This is known as the restitution condition [6]. Furthermore, a restitution hypothesis was developed by Weiss which states that decreasing the slope to < 1 could have stabilizing effects [7].

Since the restitution hypothesis was proposed, several studies, both experimental and in simulation, have been conducted to further investigate the role of restitution in electrical stability, arrhythmias and alternans [8-11]. However, there has been much debate over whether or not the restitution hypothesis is the sole predictor of stability, and some researchers suggest that stability might be multifaceted [6, 12-16]. Several studies have shown that other factors, like conduction velocity, electrotonic effects and memory [6, 12] are needed to explain alternans and arrhythmia phenomena. However it is clear that restitution is critically involved in alternans and stability of electrical activation [8-10].

Previous studies conducted to characterize the dependence of APD on previous DI have done so through the use of cycle length control. Inherent to this method is a limitation because it cannot be explicitly determined how APD depends on the previous DI without the control of the previous DI. Therefore, a real-time feedback control system, that controlled each DI, was developed [17]. Through the use of DI control, it was possible to implement a sequential oscillatory DI pacing protocol that allowed quantification of the effects of memory explicitly, i.e. hysteresis in restitution [17, 18]. The hysteresis described here is the divergence in the trajectories seen in the restitution plot of APD vs. previous DI using the DI control program previously mentioned, shown in following

figures and in previous studies [17, 18]. However, this hysteresis is not to be confused with hysteresis in stimulus intensities [19] or onset threshold of alternans [20]. Theoretically, memory (hysteresis) should have a significant impact on stability [17]. It is hypothesized that an increase in memory should lead to an increase in stability; likewise, a decrease in memory should decrease stability.

Almost equally as important as memory, if not more so, is calcium handling in the heart. Several studies have shown that calcium handling has impacted alternans and stability significantly [14, 21, 22]. Therefore we decided to alter two calcium parameters, free intracellular calcium and the L-type calcium channel current, and observe their effects on hysteresis in restitution of APD.

These studies were carried out using right ventricular endocardial porcine tissue in vitro. Free intracellular calcium was altered using BAPTA-AM, and the L-type calcium channel current was decreased using verapamil. In order to understand and explain our experimental results, we used simulations that were conducted at the conclusion of the experimental part of the study. The mathematical model used for these simulations was the canine ventricular myocyte (CVM) model developed by Fox et al [21].

Chapter Two: Background

As stated in the introduction, a heartbeat is made up of two functions: systole and diastole. Systole refers to the contraction of the heart due to the electrical occurrence of action potentials in each myocyte, whereas diastole is simply the resting phase of a heart beat associated with a diastolic interval.

Electrical conduction path and ventricular myocyte morphology:

The electrical conduction path of a heartbeat begins in the sinoatrial (SA) node, moves down through the atria, which in turn stimulates the atrioventricular (AV) node. From there the stimulus propagates through the bundle of His to the Purkinje fibers where the ventricles are stimulated. The individual ventricular cells, or ventricular myocytes, as well as other non-pacemaking cells, have a different action potential morphology than those seen in pacemaking cells [23].

A non-pacemaker cardiac cell action potential consists of five phases (0-4) as shown in figure 1. Phase 0, by far the shortest phase, refers to the depolarization of the myocyte. This depolarization is solely dependant on sodium, a positive monovalent ion, which rushes into the cell through fast sodium channels, causing the internal voltage of the myocyte to become more positive. Following the depolarization is phase 1, where all fast sodium channels are inactivated, a small amount of potassium leaks out of the cell and chloride leaks in, thus causing a transient outward current, or I_{to}. This exchange of ions causes the cell to become slightly less positive and only lasts for a few milliseconds. Subsequently is phase 2, also known as the plateau phase, which is by far the longest in duration, typically lasting around 200-400 msec. The plateau phase occurs because the L-type calcium channel current, I_{CaL}, brings calcium into the myocyte while the slow delayed rectifier potassium channel current, I_{Ks}, exudes potassium. These opposing currents somewhat create a balance in membrane potential. As the L-type calcium channels start to deactivate, the plateau tapers off because the slow delayed rectifier potassium channels are still open, causing potassium ions to flow out of the cell, making the potential rapidly more negative, which is known as phase 3. The last phase, phase 4,

refers to the cell in resting membrane potential, usually around -85 mV. This cycle is repeated when the myocyte receives an outside stimulus [23, 24].
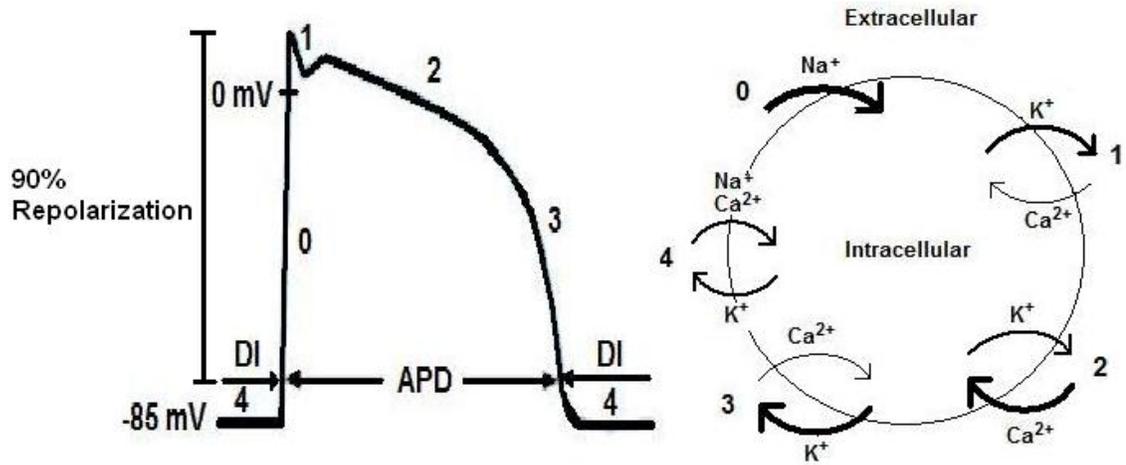
Figure 1.   Example of an action potential that depicts an APD, DI and 90% repolarization. Also shown are the currents responsible for the different phases of an action potential [24].

Calcium cycling and other calcium currents seen in the heart:

Calcium is mostly responsible for the action potential duration and is so through several different mechanisms.   During resting membrane potential, the calcium ionic concentration is larger in the extracellular space than in the intracellular space. When the extracellular voltage has reached a threshold, which is more positive than resting membrane potential, transmembrane L-type calcium channels, located on the t-tubules, are activated causing an influx of calcium ions or I_{CaL}. Some of these calcium ions then attach themselves to the sarcoplasmic reticulum, via the Ryanodine receptors attached to the junctional sarcoplasmic reticulum (JSR), causing a calcium-induced calcium-release (CICR).   The influx of calcium through the L-type (Long-lasting) calcium channel current, I_{CaL}, makes up roughly 25% of the free intracellular calcium (Ca_i) during an activation [23]. The other 75% comes from the release of calcium through the JSR. The sodium/calcium exchanger current, I_{NaCa}, also incrementally adds to the free intracellular calcium during the overshoot between phase 0 and 1. When the membrane potential is very positive, the sodium/calcium exchanger briefly acts in the "reverse mode" adding

one calcium ion and removing three sodium ions, creating a slightly less positive potential. However, the sodium calcium exchanger typically does not behave in the "reverse mode" and plays a larger role in maintaining the end of the plateau phase [23]. The free calcium then attaches to the sarcomeres, more specifically to the troponin/tropomyosin complex, causing the complex to shift, exposing a myosin binding site on the actin helix. At the same time, an ATP attaches to a myosin head causing it to shift and attach to a myosin binding site. The ATP is then released causing a contraction of the sarcomere. The process through which systole occurs on a cellular level, i.e. excitation-contraction coupling, is then complete and the calcium ions dissociate themselves and either get pumped into the network sarcoplasmic reticulum (NSR) via I_{Up}, or exit the cell via the sodium/calcium exchanger or the transmembrane calcium pump, $I_{p(Ca)}$ [23].

Other calcium currents exist besides the currents responsible for sarcolemmal contraction. An important calcium current which is only seen in, and mostly responsible for, depolarization in cardiac pacemaking cells (i.e. not ventricular myocytes) is the T-type, or transient type, calcium current, I_{CaT}. Other calcium currents that affect the amount of intracellular calcium to a lesser extent include the background calcium current $I_{Ca,b}$ and the calcium current through the sodium channel $I_{Na(Ca)}$. A schematic of currents, that increase and decrease free intracellular calcium, is shown in figure 2.
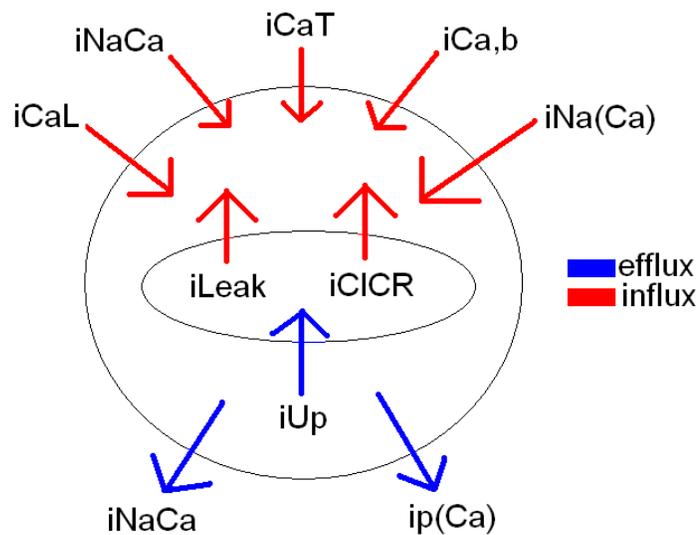
Figure 2. List of calcium currents that increase and decrease free intracellular calcium.

Verapamil:

Verapamil is a well known L-type calcium channel blocker. It has been approved by the Food and Drug Administration (FDA) since 1981. It has several brand names such as Isoptin, Verelan, Calan, Bosoptin and Covera-HS. These brands come in several doses, the most common of which are 40, 80 and 120 mg, to be administered orally, and are used to treat angina, atrial arrhythmia and hypertension. Verapamil acts as a vasodilator which aides in treatment of angina (heart pain) and essential hypertension (high blood pressure with no identifiable cause), and as a class IV antiarrhythmic agent helping atrial arrhythmias. However, there have been reported serious side effects associated with the use of this drug such as congestive heart failure (CHF), atrio-ventricular block and pulmonary edema [25].

Verapamil is listed as one of three types of L-type calcium channel antagonists, a phenylalkylamine. These three antagonists are dihydropyridines (DHPs), benzothiazepines and phenylalkylamines. All of these antagonists attach to the sixth transmembrane segment, which is seen in all four domains that make up the L-type calcium channel. Figure 3 shows a cartoon of these segments and domains, which comprise the L-type calcium channel.

7
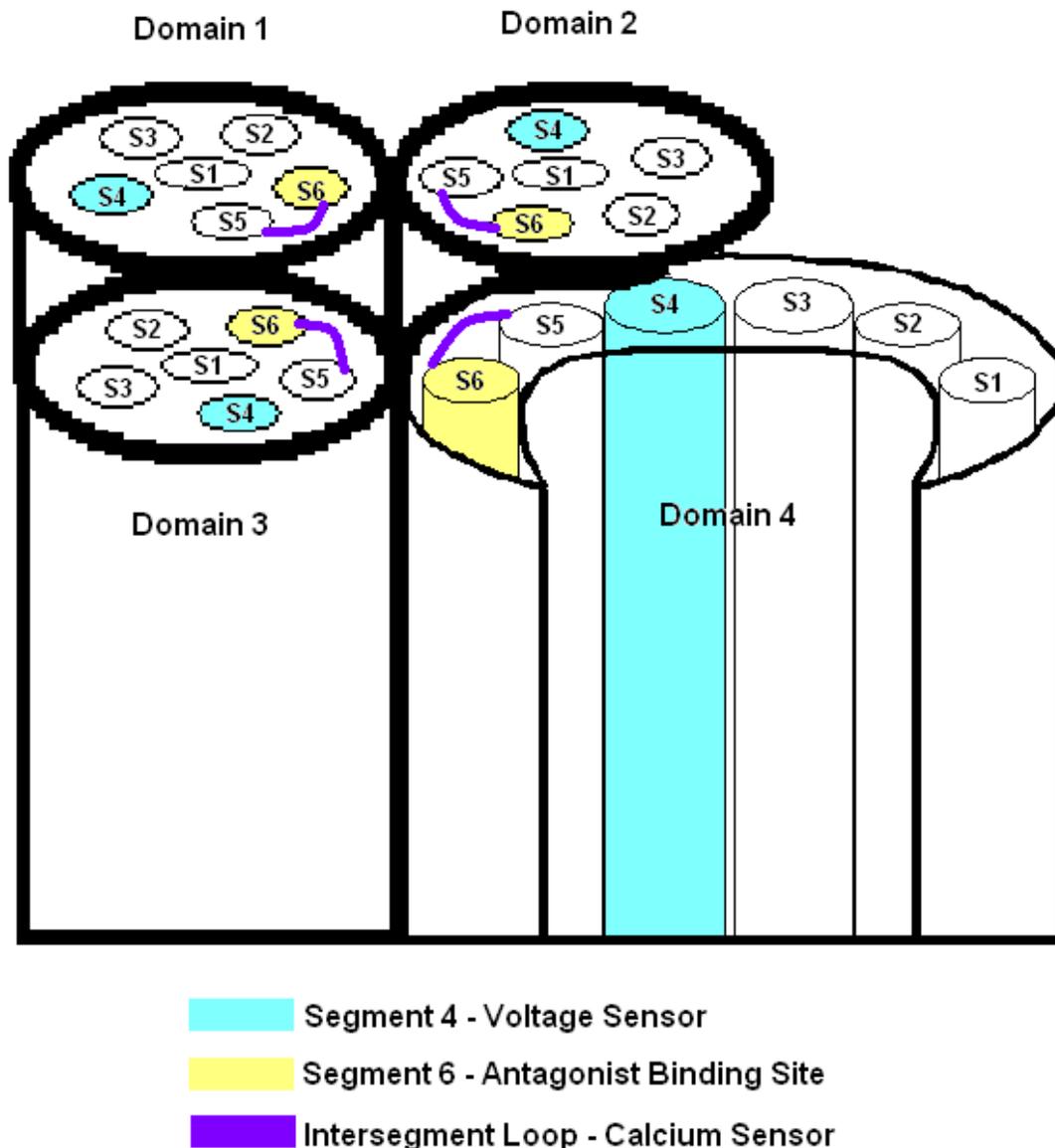
Figure 3. Shown is the L-type calcium channel which is made up of four domains each containing six transmembrane segments. The sixth segment is where the antagonists are bound [26].

BAPTA-AM:

BAPTA-AM, or 1,2-bis(o-aminophenoxy)ethane-N,N,N',N'-tetraacetic acid, tetraacetoxymethyl ester, consist of four carboxylic acid functional groups that bind two

calcium ions. This type of BAPTA is membrane permeable and, once inside the cell, is trapped in active form. The binding of BAPTA-AM to calcium ions is called chelation, and is done so with high affinity. Due to this buffering, no visible contractions were observed in isolated ventricular myocytes [14], and it has been seen in muscle fibers [27] loaded with BAPTA-AM, that the contractile force of sarcomeres was reduced, even though the intracellular calcium transient was relatively the same. It was hypothesized that BAPTA-AM decreased contractility by impeding the binding of calcium to troponin, therefore reducing the number of cross bridges [27].

In small doses of 5 µM/L, it has been noted by Leitch and Brown that BAPTA-AM can shorten APD significantly [28] and is thought to do so by a block in I_{NaCa}, yet it has also been observed by Walker et al. that, at an even smaller dose of 0.5 µM/L, baseline APD does not change with the introduction of BAPTA-AM [20]. These conflicting BAPTA results of effect on APD make it difficult to determine whether or not BAPTA is effectively chelating calcium intracellularly.

Mathematical modeling:

To explain the mechanisms behind our statistically significant results, the canine ventricular myocyte (CVM) model was chosen for our simulation studies. This model was originally created by Winslow et al. in 1999 [29]. Fox et al. further modified this model in 2001, with the addition of simple intracellular calcium dynamics and alteration of inward rectifier potassium current (I_{K1}), the rapid and slow components of the delayed rectifier potassium current (I_{Kr} and I_{Ks}) and L-type calcium current (I_{Ca}) in order to exhibit stable alternans in midmyocardial ventricular myocyetes [21]. The equations used in this model were adapted from the Winslow, LRd and Chaudin models [21].

Chapter Three: Methods and Analysis

The study conducted consisted of two parts: an experimental part which was followed by simulations using a mathematical model. The experimental part consisted of determining the effects of decrease in L-type calcium channel current through the use of verapamil and manipulation of free intracellular calcium through the use of BAPTA-AM.

Experimental part:

All experiments were conducted after obtaining approval from the Institutional Animal Care and Use Committee at the University of Kentucky and in accordance with their policies. Six farm pigs (sus scrofa) with an average weight of 18.17 kg for the verapamil study, and 18.0 kg for the BAPTA-AM study, were sedated with a telazol/ketamine/xylazine mixture (4−8 mg/kg, 2−4 mg/kg, 2−4 mg/kg) and were anesthetized with thiopental sodium (10–30 mg/kg, IV). After anesthesia, the hearts were quickly removed and placed in Tyrode's solution that was kept on ice. Immediately after explantation, a strip of right ventricular tissue, roughly 10 x 5 mm, was placed in a Plexiglass chamber, with the endocardial side facing upwards. The tissue was continuously superfused in the chamber with circulated Tyrode's solution which was gassed with 95% O_2 and 5% CO_2 and warmed to 37 ± 1 degree Centigrade and had a pH of 7.3 ± 0.05. The composition of the solution, in mmol/L, was: $MgCl_2 = 0.5$, $NaH_2PO_4 = 0.9$, $NaCl = 137$, $KCl = 4$, Glucose = 5.5, and $CaCl_2 = 2$. To this mixture $NaHCO_3$ was incrementally added until the desired pH level was achieved; the final concentration of $NaHCO_3$ was 24 mmol/L [9]. The tissue was paced at a 500 msec constant cycle length via a bi-polar platinum-iridium electrode for about an hour to achieve acclimatization. The stimulus was bi-phasic with a total duration of 6 msec. The stimulus intensity was 4-6 times the diastolic threshold.

Glass micropipettes filled with 3M KCl were used to record the trans-membrane potential (TMP) from a location within about 5 mm from the bi-polar stimulating electrode. The TMP was digitized by a commercial data acquisition system at a rate of 10,000 samples/second. The TMP was simultaneously used in a custom developed program for

real-time control of DI, as previously described [17]. Figure 4 shows a schematic representation of the setup used for our experiments. We used two protocols, both lasting 220 beats, to determine hysteresis in restitution. In both protocols, the DI was constant for the first twenty beats followed by 200 beats of sinusoidal oscillations. Each sine wave had a period of 100 beats, thus creating two full periods for each protocol. The first of the two protocols consisted of DI control in a sinusoidal pattern with a mean value equal to 400 msec and a maximum and minimum DI range between 100 and 700 msec. The second protocol was also a DI controlled sine wave, but with a mean value equal to 150 msec and a range between 10 and 290 msec. An example of each DI protocol is shown in figure 5. The sinusoidal pattern for our protocol was chosen for two reasons. The first reason was based on an observation that Goldberger and West made: people who suffered from severe cardiac pathologies had less heart rate variability (HRV) and their HRV looked very similar to that of a sinusoid [30]. Secondly, according to the mathematical Lissajous figures, the plotting of a sinusoid (i.e. DI) versus a sinusoid (i.e. APD) produces a loop, in our case, a hysteresis loop. These protocols were executed at least three times each. Between trials, the tissue was paced at 500 msec cycle length for about five minutes.
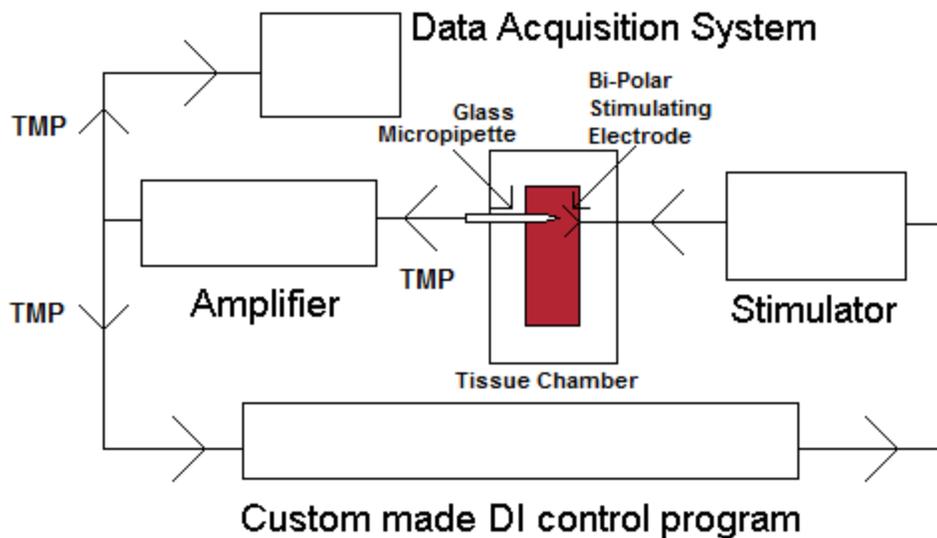
Figure 4. Schematic representation of the equipment-based setup of data acquisition and DI control used for experiments.
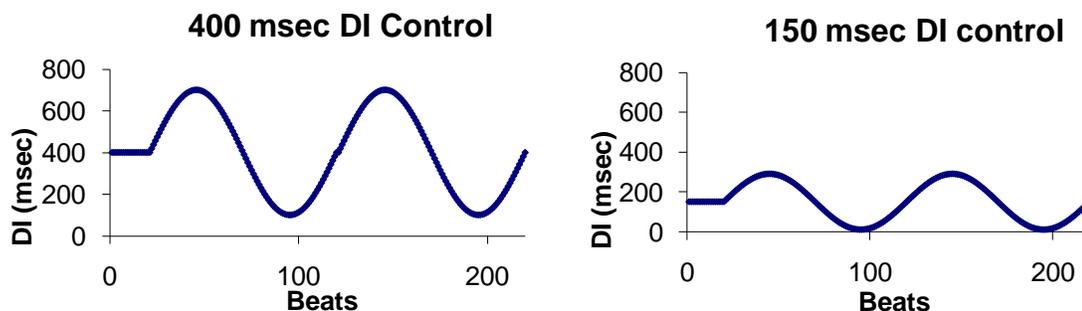
Figure 5. Examples of the 400 msec mean DI protocol and 150 msec mean DI protocol used in the experiments.

After all control, i.e. pre manipulation, recordings were obtained, the buffer was switched to one with the same composition as described above but with the addition of a drug, depending on which experiment (I_{CaL} or Ca_i) was being conducted. Verapamil (Tocris Bioscience) at a concentration of 2 μM/L (or 1 mg/L) was added to the Tyrode's solution to decrease the L-type calcium channel current. Similarly, for free intracellular calcium

12

chelation 0.5 µM/L (or 0.38 mg/L) of BAPTA-AM was added to the Tyrode's solution. However, BAPTA-AM is not soluble in water; therefore, we mixed 10 mg of BAPTA-AM with 10 mL of DMSO to create a solution with 1 mg/mL of BAPTA-AM in DMSO. From this solution we took 0.38 ml and added it to 1 Liter of Tyrode's solution, thus giving the desired concentration. The tissue adapted for roughly one hour after switching to the buffer containing the drug. BAPTA-AM was protected from light and moisture while in storage, and during circulation, i.e. during loading, the ambient light in the working area was decreased as much as possible. After acclimation the protocols mentioned above were repeated.

From the digitized TMP recordings, APDs and DIs were calculated using a constant threshold method. The threshold was defined at 90% repolarization, i.e. 90% of the difference between the maximum amplitude of the first action potential and resting membrane potential, for each recording (shown in figure 1). Analyses were conducted off-line on the recorded TMPs using custom developed Matlab code (The Mathworks Inc.).

Figure 6 depicts hysteresis in restitution of APD as created by the sequential and oscillatory DI control changes. This phenomenon has been demonstrated in another species, i.e. in canines [17], as well as in simulations [18]. From the APD versus previous DI curves, loop area, thickness (defined as the difference between APDs at the mean value of DI, i.e. at DI = 400 and = 150 msec for the two protocols), max delay (defined as the delay between when DI reached its maximum and when the APD reached its maximum, measured in beats), min delay (defined as the delay between when DI reached its minimum and when the APD reached its minimum, measured in beats), and overall tilt (defined as the slope of a line connecting the maximum and minimum APD vertices) were calculated. In some trials, because of the switch to constant DI pacing from constant cycle length pacing, the hysteresis loop created by the first sinusoid had an underlying baseline shift due to slow APD adaptation. Our focus was on effects of L-type calcium current and free intracellular calcium concentrations on hysteresis, which is a feature of memory. Therefore, we computed these measures of hysteresis from the

second sinusoidal oscillation, which was not affected as much by the APD adaptation. On rare occasions (about 0.18% incidence), the real time DI control was transiently lost for one or two beats. When this occurred, the missed DIs, and corresponding APDs, were replaced by the average of the preceding and succeeding values. The calculated parameters - average APDs, average DIs, standard error of the mean (SEM), normalized APDs and normalized SEM (all of which were used in creating the hysteresis loop figures), as well as area, loop thickness, overall tilt, max and min delay - that were obtained during multiple trials of the same protocol, were first averaged within each animal and then averaged across animals. A paired t-test across the means was used to test differences before and after I_{CaL} manipulation as well as free intracellular calcium concentration manipulation. Statistical significance was accepted when $p \leq 0.05$.
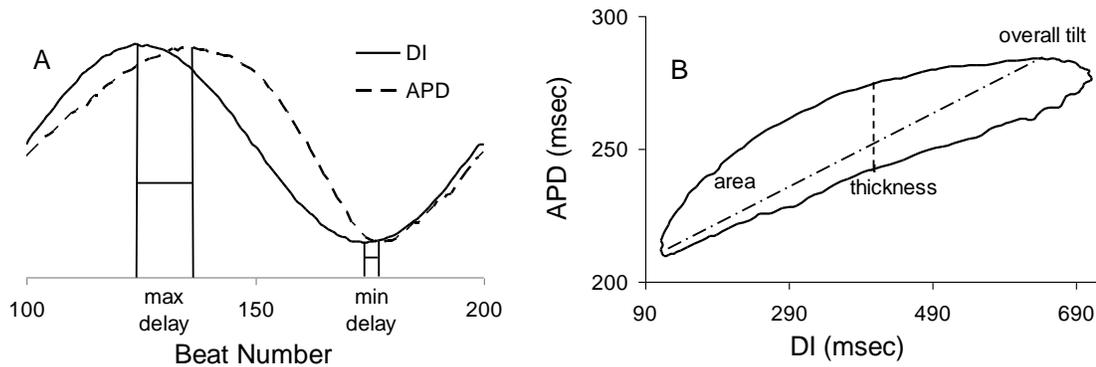
Figure 6. (A) DIs and APDs produced during last 100 beats of sinusoidal protocol. The APDs have been scaled and vertically shifted to better show the maximum and minimum delays between APD and DI at peak and nadir values. (B) Hysteresis in restitution corresponding to the APD vs. preceding DI values in panel A. Overall tilt is defined as the slope between the maximum and minimum APD vertices. Thickness was defined as the change in APD at the mean DI value. Area is defined as the area enclosed by the loop.

Simulation study for I_{CaL}:

As the results section will show, the changes in hysteresis upon administration of BAPTA-AM were insignificant, therefore the simulation part of our study focused on manipulation of I_{CaL} only. Simulations were conducted using the canine ventricular

14

myocyte (CVM) model developed by Fox et al. [21] in order to interpret and understand the observed changes in hysteresis upon administration of verapamil. The model was implemented using programs developed in house. The DI control simulations were conducted in a single cell. Both 400 and 150 msec mean value protocols were simulated with the exception that these protocols were previously paced with 100 beats of constant DI control, as opposed to the 20 used in experiments, to better achieve APD accommodation. Both protocols were simulated with the nominal value of I_{CaL} (equivalent to pre manipulation, i.e. control) and with altered I_{CaL}. The L-type calcium current was manipulated by multiplying the calculated current by a scaling factor, where the current was decreased in steps of 10 percent of the nominal value (i.e. post manipulation). The currents, I_{CaL} and I_{NaCa}, computed from the model were integrated over each beat, i.e. over each activation, whereas the calcium concentrations, free intracellular calcium, Ca_i, and calcium in the sarcoplasmic reticulum (SRCa), were computed from their peak values obtained within each beat in order to obtain insight into mechanisms that could result in the changes that we observed in the experimental part of the verapamil study.

Chapter Four: Results

A hysteresis loop was observed in all trials when the DIs changed sequentially in a sinusoidal sequence, which has been demonstrated in previously reported observations in canines [17] and in simulations [18].

Manipulation of L-type calcium channel:

After verapamil had been administered, the average APDs recorded during 500 msec cycle length pacing, changed from 245 to 196 msec, which is a 20% decrease and statistically significant at $p < 0.05$. Figure 7 shows samples of action potentials recorded during one trial before (pre) and after (post) I_{CaL} manipulation. As expected, and depicted, the post manipulation plateau phase was lessened. From the computed APD and DI, restitution relationships were determined as a function between a DI and the succeeding APD. Figure 8 shows the average (N=6) of restitution relationships (i.e. hysteresis loops) pre and post manipulation for both the 400 and 150 msec protocols. As stated in the methods section, restitution relationships were first averaged within each pig and then across all pigs. For the ease of visualization, in figure 8, the post manipulation hysteresis loops are offset vertically, thus visually removing the effects of changes in baseline APD, and horizontally, removing the minor differences in DI control mostly due to differences in conduction velocity delay. The vertical offset was about 36 msec for the 400 msec mean DI protocol and about 30 msec for the 150 msec mean DI protocol. The horizontal shift was 5 msec for the 400 msec protocol and 3 msec for the 150 msec protocol. These offsets were only used to make these figures, and were not used in calculation of any of the parameters of hysteresis.
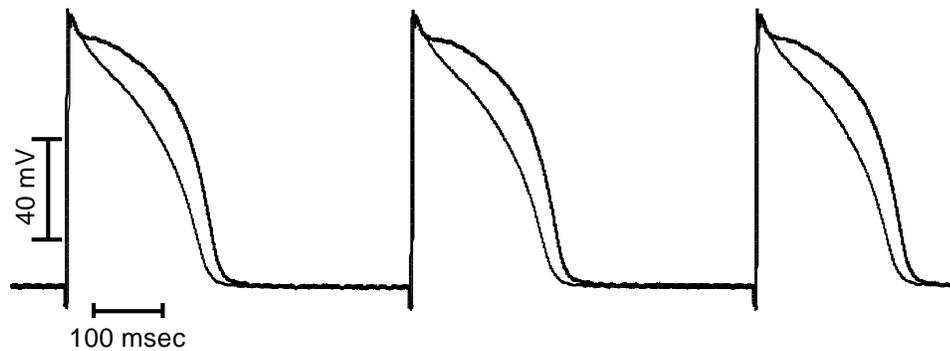
Figure 7. Examples of TMPs recorded during one trial before (thick) and after (thin) verapamil during 500 msec cycle length pacing. The traces are aligned to better show the differences.
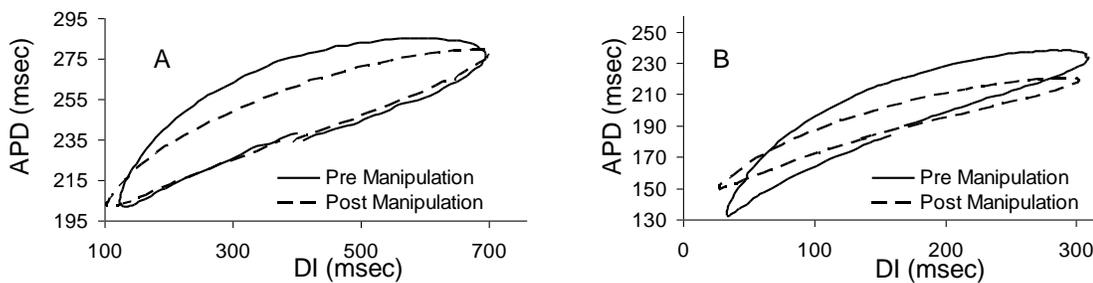
Figure 8. Averaged (N=6) hysteresis loops, pre and post verapamil for 400 msec protocol (A) and 150 msec protocol (B). The post manipulation curves are vertically and horizontally offset to facilitate comparison with pre manipulation curves.

The restitution relationships shown in figure 8 are graphed without error bars to better portray the average effects of verapamil. Figure 9 shows the average relationships with error bars representing the standard errors of mean (SEM). The error bars in figure 9 somewhat overstate the degree of variation in the restitution characteristics across the pigs used in our experiments because they are largely influenced by the differences in baseline APDs among different pigs. Thus the error bars do not accurately represent the variation in the degree of hysteresis of restitution. In order to better show the variation in characteristics of restitution across all pigs, we normalized the restitution relationships within each pig such that the maximum and minimum change in APD was between +1

and -1. The normalized relationships were then averaged across all pigs. These averages with the normalized standard errors of mean are shown in figure 10. Figure 10 shows that the hysteresis loops were highly reproducible across animals during both pre and post manipulation for both protocols. The maximum standard errors for the normalized loops were ±0.07 (3.5%) for the 400 msec protocol and ±0.09 (4.5%) for the 150 msec protocol.
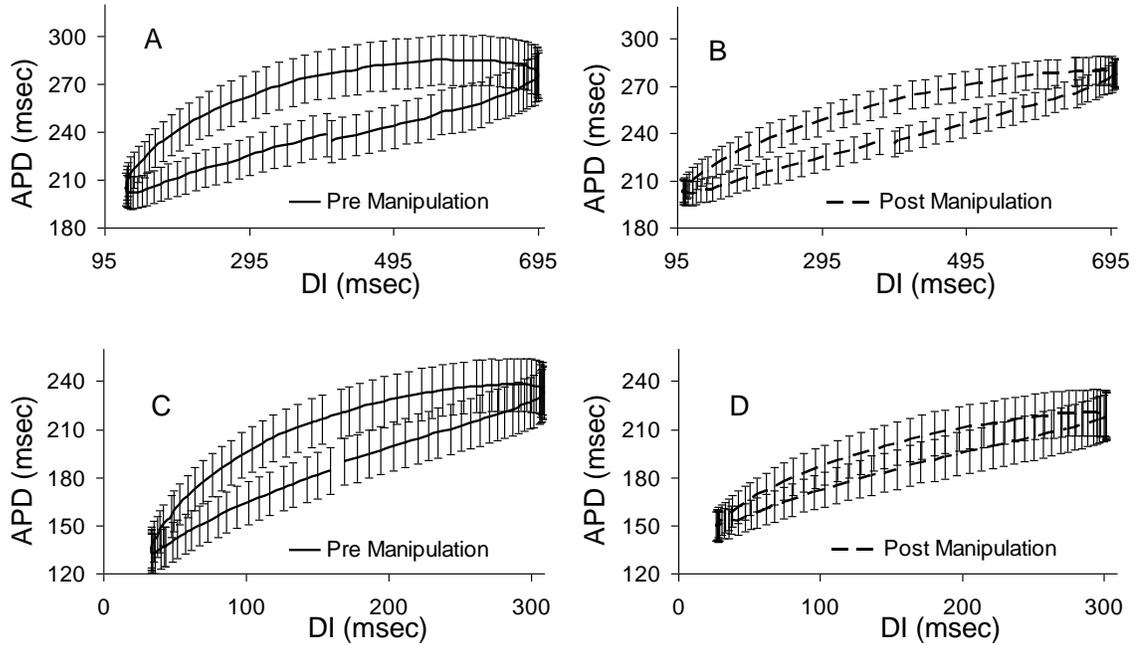
Figure 9. Average (N=6) of hysteresis loops (±SEM) for 400 msec protocol pre (A) and post verapamil manipulation (B); 150 msec protocol pre (C) and post verapamil manipulation (D).
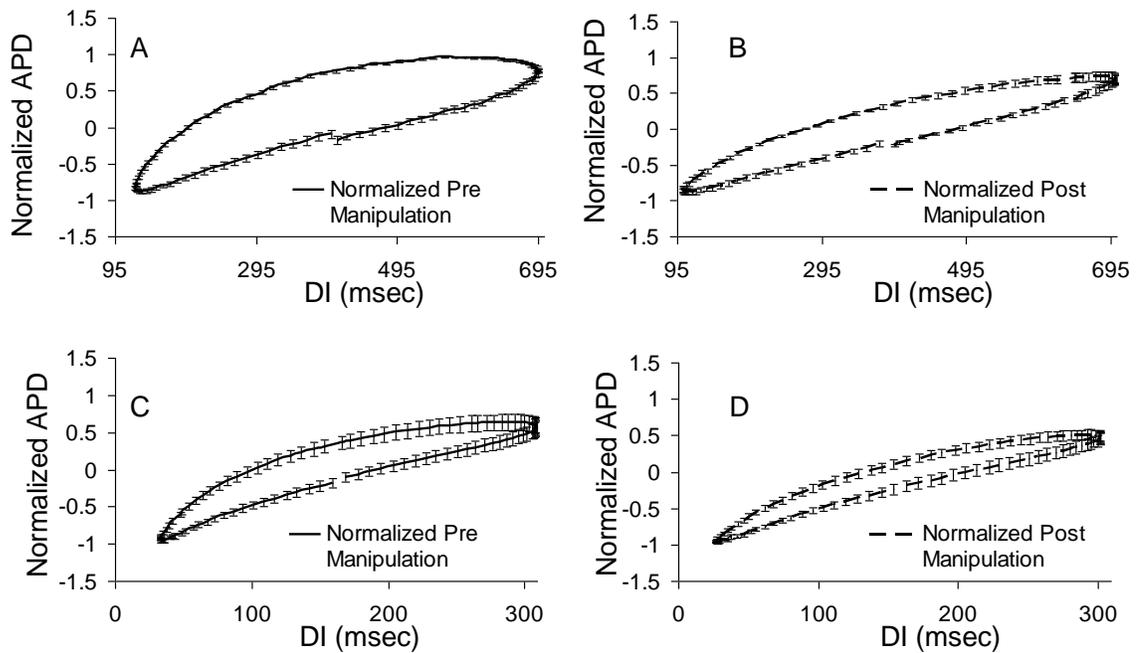
Figure 10. Average (N=6) of normalized hysteresis loops (±SEM) for 400 msec protocol pre (A) and post verapamil manipulation (B); 150 msec protocol pre (C) and post verapamil manipulation (D).

The quantitative measures of restitution were computed from the averaged relationships within each animal for each of the two protocols to obtain one measure per animal per protocol. These measures were then averaged across all six animals. These results are shown in table 1. Included in this table are the averages (± SEM) pre and post manipulation, as well as the absolute changes (i.e. total change) and percent changes. The percent differences were calculated as the difference, post minus pre, divided by the pre manipulation value.

Table 1. Quantitative measures of restitution relationships of averaged ± SEM values (N=6), total change and percentage, for both the 400 msec and 150 msec protocols in verapamil study. Shown are area, thickness, overall tilt, max delay and min delay computed during pre and post verapamil manipulation. * $p \leq 0.05$.

	400 msec protocol			
	Pre Manipulation Mean	Post Manipulation Mean	Total Change	Percentage (%)
Area (msec2)	19310 ± 902	12061 ± 858*	-7249	-38
Thickness (msec)	40.2 ± 2.1	26.9 ± 2.1*	-13.3	-33
Overall Tilt	0.18 ± 0.02	0.14 ± 0.01*	-0.04	-22
Max Delay (beats)	13.7 ± 0.99	5.3 ± 0.54*	-8.4	-61
Min Delay (beats)	4.8 ± 0.25	3.2 ± 0.57*	-1.6	-33

	150 msec protocol			
	Pre Manipulation Mean	Post Manipulation Mean	Total Change	Percentage (%)
Area (msec2)	7184 ± 552	3566 ± 246*	-3618	-50
Thickness (msec)	34.3 ± 2.3	17.2 ± 1.4*	-17.1	-50
Overall Tilt	0.42 ± 0.02	0.28 ± 0.03*	-0.14	-33
Max Delay (beats)	8 ± 0.85	6.1 ± 0.5	-1.9	-24
Min Delay (beats)	3.2 ± 0.76	2.6 ± 0.52	-0.6	-19

As table 1 shows, all parameters decreased after verapamil was introduced. Generally, the degree of decrease was larger for the 150 msec protocol. The statistically significant changes, as seen in both the 400 msec and 150 msec protocols respectively, were a decrease in area of about 38% and 50%, decrease in overall tilt of 22% and 33% and in thickness of about 33% and 50%.

To further our understanding of potential mechanisms by which verapamil could alter hysteresis, we conducted simulations using the CVM model. The decrease in I_{CaL} was simulated by scaling the computed current downward via a multiplying factor. Figure 11 shows results of simulations in terms of peak intracellular calcium during each beat, i.e. Ca_i (maximal), L-type calcium channel current I_{CaL} (integrated over a beat), maximum sarcoplasmic reticulum calcium (SRCa) content during a beat and integrated (over a beat) sodium calcium exchanger current I_{NaCa}. Results shown in figure 11 are for the 400 msec

protocol during nominal, equivalent to pre manipulation, I_{CaL}, and during a 61.75% decrease in I_{CaL} (i.e. when the current was reduced to 38.25% of the nominal value). This value was chosen because the decrease in loop thickness in simulations, at this level of I_{CaL}, matched the decrease observed experimentally during the 400 msec protocol, which was 33%. Figure 11A shows that at both the 100th and the 150th beat, the value of DI was equal to 400 msec. The difference between these two points is that the DIs at the 100th beat were increasing, while at the 150th beat they were decreasing. The numerical values of the above stated results of calcium currents and concentration at these two beats are provided in table 2. The results in table 2 illustrate the asymmetry seen in calcium handling even though the value of DI at these two points was the same. The CVM did not produce changes equal to those seen experimentally in all parameters of hysteresis for any one level of reduction in I_{CaL}. Different levels of reductions of I_{CaL} were required in the model to produce changes in different parameters of hysteresis similar to those observed experimentally. To produce a decrease in overall tilt for the 400 msec protocol in simulations equal to the average decrease observed during experiments, a decrease in I_{CaL} of about 41% of the nominal value was required. Likewise, to match the experimental loop area decrease, I_{CaL} had to be decreased by about 37% of the nominal value. However, there were no simulation values that matched the max and min delay results seen in experiments for the 400 msec protocol. For the 150 msec protocol, matching decreases in area, thickness, overall tilt, and max delay required decreasing the L-type calcium channel current in the simulation by roughly 57%, 56%, 72% and 51% of the nominal value, respectively. No simulation results matched what was seen experimentally for the min delay in the 150 msec protocol.

Table 2. The values of the points (A-P) corresponding to figure 11. These points correlate to the 100th and 150th beat in sinusoidal 400 msec protocol. The DI values at these beats are the same, and are equal to the mean DI (400 msec). The differences between each set of points are also shown to depict asymmetry.

	Point	Value	Difference
Cai (nominal I_{CaL})	A	1.53	
	B	1.91	-0.38
Cai (reduced I_{CaL})	C	0.71	
	D	0.86	-0.15
i_{Ca-L} (nominal I_{CaL})	G	-43.75	
	H	-41.80	-1.95
i_{Ca-L} (reduced I_{CaL})	E	-16.02	
	F	-15.89	-0.13
SRCa (nominal I_{CaL})	I	347.55	
	J	368.33	-20.78
SRCa (reduced I_{CaL})	K	286.86	
	L	301.50	-14.64
i_{NaCa} (nominal I_{CaL})	O	-18.44	
	P	-25.02	6.57
i_{NaCa} (reduced I_{CaL})	M	-8.39	
	N	-12.36	3.97
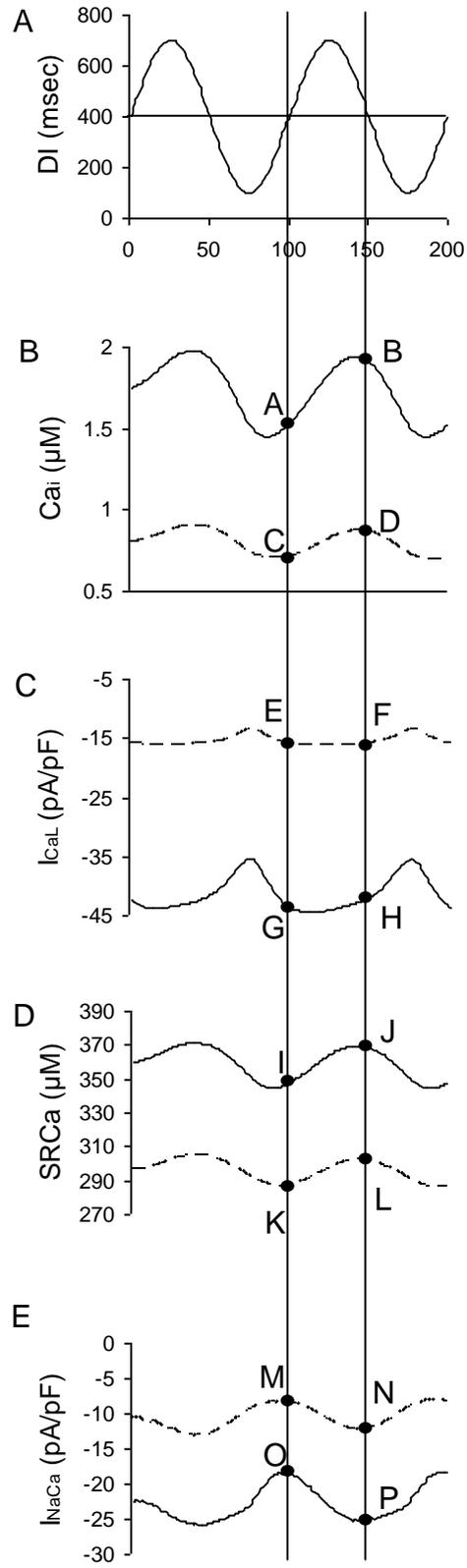
Figure 11. Results of simulation of the 400 msec protocol. A) The values of DI, B) maximal concentration of calcium, Ca_i, C) integrated L-type calcium channel current, I_{CaL}, D) maximal sarcoplasmic reticulum calcium content (SRCa) and E) integrated sodium calcium exchanger current, I_{NaCa}. Each parameter was calculated over each beat. Note that for I_{CaL} and I_{NaCa}, larger negative values denotes larger integrated currents. Shown are results with nominal I_{CaL} (solid lines) and reduced I_{CaL} (dashed).

Manipulation of free intracellular calcium:

After the administration of BAPTA-AM, the average APDs recorded during 500 msec cycle length pacing, were essentially unchanged (from 265 msec to 267 msec - a 0.53% increase). This increase was statistically not significant and it can be concluded that this change was not consequential. Figure 12 shows samples of action potentials recorded during one trial pre and post Ca_i manipulation. The action potentials after manipulation of Ca_i showed no significant change. Similar to the figures and computations described above for verapamil part of the study, restitution relationships were also determined for the studies conducted using BAPTA-AM. Figure 13 shows the average (N=6) of restitution relationships (i.e. hysteresis loops) pre and post manipulation for both the 400 and 150 msec protocols. For the ease of visualization, the post manipulation hysteresis loops were offset vertically and horizontally in the same manner as the verapamil analysis. The vertical offset was about 4 msec for the 400 msec mean DI protocol and about 8 msec for the 150 msec mean DI protocol. The horizontal shift was 9 msec for both the 400 msec protocol and the 150 msec protocol. These offsets were only used to make these figures, and were not used in parameters of hysteresis calculation.
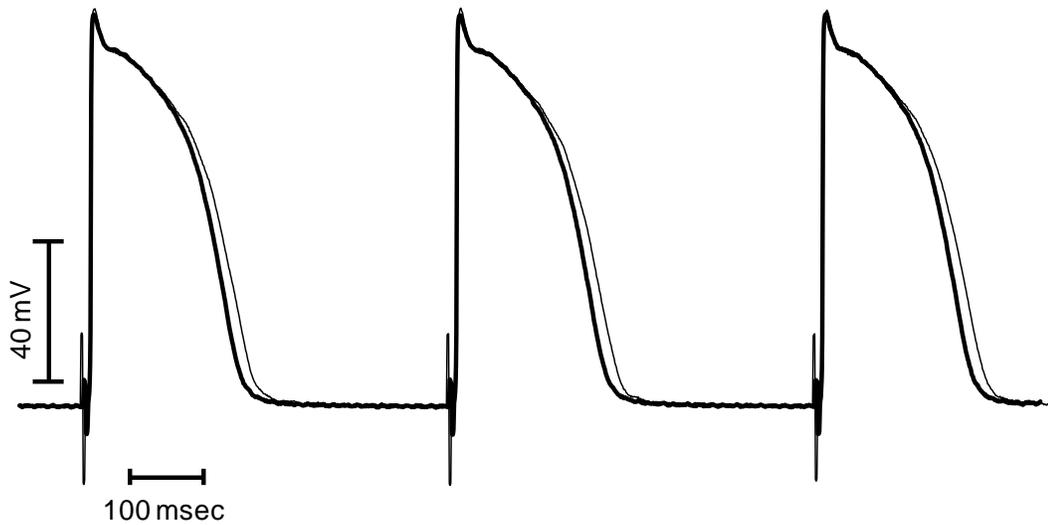
Figure 12. Examples of transmembrane potentials recorded during one trial before (thick) and after (thin) BAPTA-AM during 500 msec cycle length pacing. The traces are aligned, and the post manipulation curve is scaled up by 4%, to better show the differences.
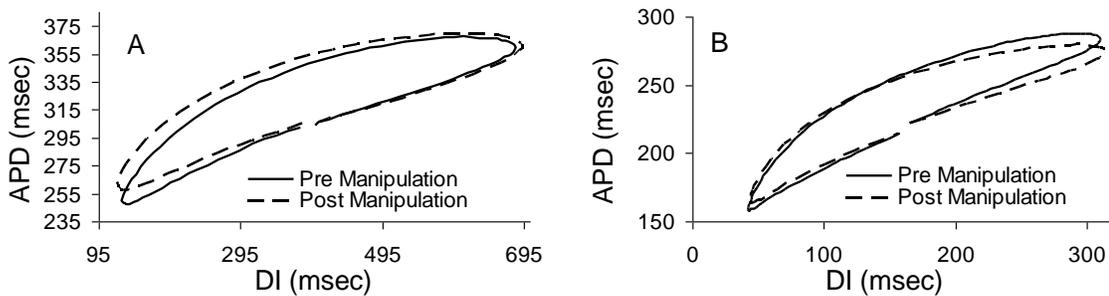
Figure 13. Averaged (N=6) hysteresis loops, pre and post BAPTA-AM for 400 msec protocol (A) and 150 msec protocol (B). The post manipulation curves are vertically and horizontally offset to facilitate comparison with pre manipulation curves.

Similarly, the restitution relationships, shown in figure 13, are graphed without error bars to better portray the average effects of BAPTA-AM. Therefore, figure 14 shows the average relationships with error bars representing the standard errors of mean (SEM).

26

The error bars in figure 14 also overstate the degree of variation in restitution characteristics across the pigs used in our experiments because they too are largely influenced by the differences in baseline APDs among different pigs. Thus the error bars do not accurately represent the variation in the degree of hysteresis of restitution. In order to better show the variation in characteristics of restitution across all pigs, we normalized the restitution relationships within each pig such that the maximum and minimum change in APD was between +1 and -1. The normalized relationships were then averaged across all pigs. These averages with the normalized standard errors of mean are shown in figure 15. Figure 15 shows that the hysteresis loops were highly reproducible across animals during both pre and post manipulation for both protocols. The maximum standard errors for the normalized loops were ±0.04 (2%) and ±0.07 (3.5%) for the 400 and 150 msec protocols, respectively.
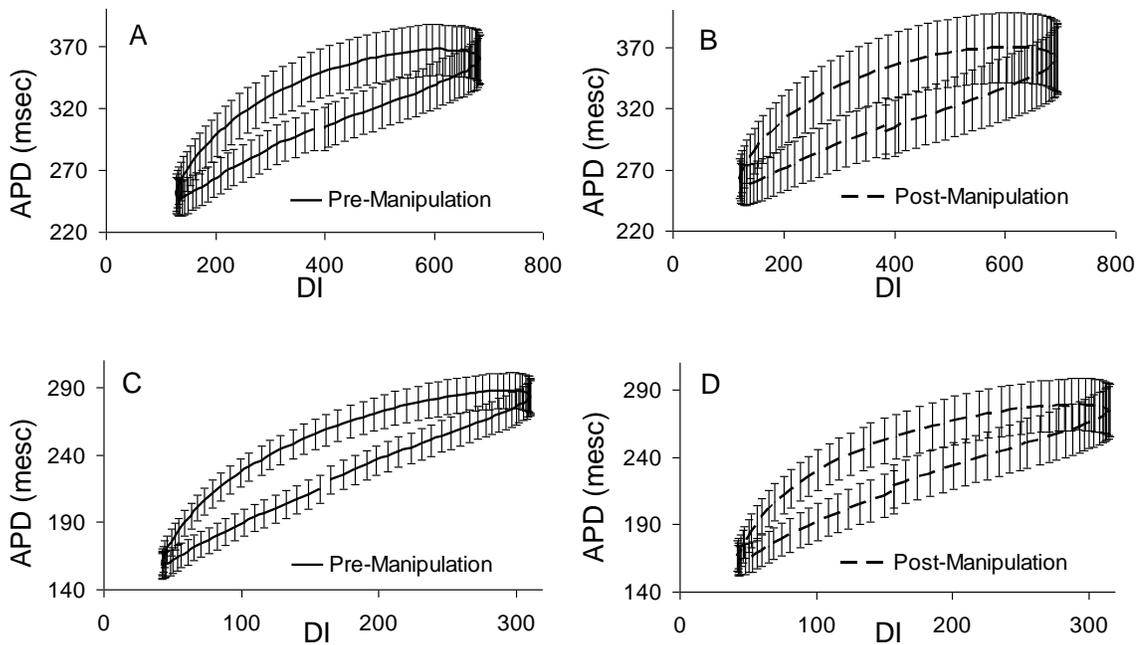
Figure 14. Average (N=6) of hysteresis loops (±SEM) for 400 msec protocol pre (A) and post BAPTA-AM manipulation (B); 150 msec protocol pre (C) and post BAPTA-AM manipulation (D).
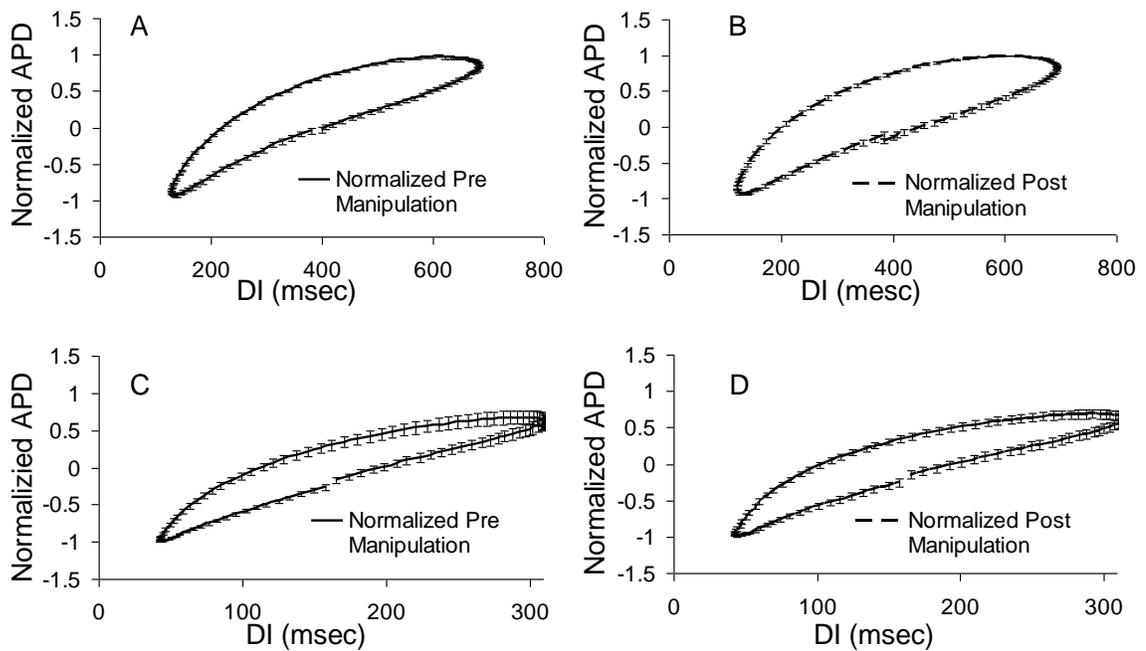
Figure 15. Average (N=6) of normalized hysteresis loops (±SEM) for 400 msec protocol pre (A) and post BAPTA-AM manipulation (B); 150 msec protocol pre (C) and post BAPTA-AM manipulation (D).

The quantitative measures of restitution were computed from the averaged relationships within each animal for each of the two protocols to obtain one measure per animal per protocol. These measures were then averaged across all six animals. These results are shown in table 3. Included in this table are the averages (± SEM) of pre and post manipulation for each measure, as well as the absolute and percent changes. Similar to the verapamil analysis, the percent differences were calculated as the difference, post minus pre, divided by the pre manipulation value.

Table 3. Quantitative measures of restitution relationships of averaged ± SEM values (N=6), total change and percentage, for both the 400 msec and 150 msec protocols in BAPTA-AM study. Shown are area, overall tilt, thickness, max delay, and min delay computed during pre and post manipulation. None of the changes were statistically significant at the level of $p < 0.05$.

	400 msec protocol			
	Pre Manipulation Mean	Post Manipulation Mean	Total Change	Percentage (%)
Area (msec2)	21645 ± 2250	23803 ± 2556	2158	10
Thickness (msec)	46.2 ± 4.9	50.1 ± 5.4	3.9	8
Overall Tilt	0.24 ± 0.02	0.23 ± 0.02	-0.04	-4
Max Delay (beats)	11.8 ± 0.3	13.3 ± 0.8	1.5	13
Min Delay (beats)	3.4 ± 0.4	4.3 ± 0.3	0.9	27

	150 msec protocol			
	Pre Manipulation Mean	Post Manipulation Mean	Total Change	Percentage (%)
Area (msec2)	8890 ± 978	8260 ± 763	-630	-7
Thickness (msec)	42.6 ± 4.5	39.3 ± 3.6	-3.3	-8
Overall Tilt	0.51 ± 0.04	0.47 ± 0.04	-0.04	-8
Max Delay (beats)	7.8 ± 0.5	8.5 ± 0.3	0.7	9
Min Delay (beats)	2.7 ± 0.4	4.1 ± 1.1	1.4	52

As table 3 shows, the area, thickness, max and min delay saw an increase and overall tilt a decrease for the 400 msec DI control protocol; whereas area, thickness, and overall tilt showed a decrease, and max and min delay increased in the 150 msec protocol. None of these parameters were determined statistically significant by the t-test.

Chapter Five: Discussion

Restitution, or the dependence of an APD on previous DI, has and continues to be a main focus in several studies because of its widely believed link with alternans and arrhythmia [8-10, 31-33]. In addition to this dependence, memory also is thought to affect stability significantly [6, 17, 34]. In this context, memory is defined as the dependence of an APD on, not one, but several previous DIs and APDs [34]. Recently, there have been an increasing number of studies suggesting that intracellular calcium handling may also impact stability importantly [14, 21, 22]. With both aspects in mind, our purpose in the present study was to determine the effects of a prominent component of change in intracellular calcium, the L-type calcium current I_{CaL}, as well as the chelation of free intracellular calcium, on restitution and memory in APD.

Manipulation of L-type calcium channel:

Our study shows that through a decrease of I_{CaL} produced by the use of verapamil, measures of memory, as quantified by the changes in the parameters of hysteresis in restitution of APD, decreased (i.e. loop thickness, area, overall tilt, max delay and min delay). Previously, it has been predicted by others, using the restitution hypothesis, that verapamil would have a stabilizing effect since it decreases the slope of restitution [35, 36]. In our study, we did not calculate the slope as defined by the standard or dynamic protocol. However, the overall tilt can be loosely considered to be an analog of "slope", noting that in our case, the restitution is obtained when DIs change in sequence, while in the previous studies, cycle lengths changed and non-sequential APD and DI pairs were mapped. Despite this significant difference, the overall tilt of the hysteresis loop also decreased after the use of verapamil, which is consistent with the decreases in slopes as seen by others [35, 36]. However, if, as predicted by theory [6, 17, 34], memory does increase stability, then the decrease in all of the measures of memory would suggest that the decrease in I_{CaL} may not increase stability as predicted by the restitution hypothesis alone. Therefore, our results could provide an explanation for the paradoxical observations seen in studies that show verapamil does not necessarily increase stability [37-39], even though verapamil may flatten the slope of restitution. These divergent

results also demonstrate that use of sequential changes in DI, as seen in the sinusoidal protocols, can reveal additional features of the dynamics of APD than those revealed by protocols using non-sequential changes to map restitution as is the case with the contemporary protocols [9, 40, 41].

The purpose in the use of the CVM model, as stated in the methods section, was to simulate changes in parameters of hysteresis which were observed in experiments and to understand the mechanisms behind the observed changes. Previously, studies have been conducted where hysteresis was shown in canines [17]. Pigs were used in this study for two reasons: to show that hysteresis in restitution exists in other mammals, besides canines, and because several pig studies have been conducted that explore related phenomena, such as effects of memory and restitution on stability [12, 42]. Although the CVM model is modeled after a canine, and we used pigs experimentally, we believe that the use of this model was sufficient, as the hysteresis loops seen experimentally in canines and pigs were similar.

The results of simulations, in figure 11 and table 2, provide some insight on the possible mechanisms of the asymmetry that occurs at the same DI between the ascending and the descending phases. We believe this asymmetry seen in Ca_i, I_{CaL}, I_{NaCa}, and SRCa, among others, contributes significantly to hysteresis and thus memory. Figure 11 shows that the amount of calcium in the sarcoplasmic reticulum is larger during the descending phase than the ascending phase. This difference occurs because, during the descending phase, each activation is preceded by a larger DI, providing more recovery time for calcium [23], and thus higher SR Ca stores. This increase in the SR calcium causes an increased release during calcium induced calcium release (CICR) leading to an increased Ca_i. The increased Ca_i, in turn, increases the sodium/calcium exchanger current while, conversely, the I_{CaL} begins to decrease (figure 11C). Opposite findings are seen during the ascending phase. The APDs during the descending phase were larger than the ascending phase, which could indicate that the sodium/calcium exchanger current dominated the negative feedback of Ca_i on I_{CaL}. This asymmetry in currents and concentrations leads to a difference in APD at the same DI value resulting in the hysteresis loop.

31

In order to determine a possible explanation for which changes in I_{CaL} would decrease memory, the current in the model was altered until the decrease in the simulated hysteresis loop thickness matched the decrease in loop thickness seen during experiment, which was 33% for the 400 msec protocol. A reduction of I_{CaL} by 61.75% from the nominal value, or to 38.25% of the nominal value, resulted in a similar decrease in loop thickness. The effects of this decrease on calcium currents, I_{CaL} and IN_{aCa}, and concentrations, Ca_i and SRCa, are shown in figure 11 (dashed lines). As expected, these results show similar, but diminished in magnitude, trajectories of the currents and concentrations. As a result, the difference between the APDs of the ascending and descending phases, and thus loop thickness, was also smaller. We consider that these decreases in the degree of asymmetry across all parameters observed in simulations contributed to a decrease in the hysteresis loop parameters.

Bi-directional coupling between membrane potential and Ca_i has been the focus of several recent studies and is another important link between calcium handling within the cell and changes in APD [43, 44]. Bi-directional coupling is the dependence of the membrane potential voltage on intracellular calcium and vice versa. Critical to this coupling is the relative dominance between two components: the reduction in L-type calcium current and the increase in the sodium/calcium exchanger current due to increased intracellular calcium. To determine the contribution of this coupling, and the dominating current in the case of sinusoidal changes in DI with the CVM model, we removed the asymmetry imposed by oscillating DIs. This was completed by running a constant DI control protocol with beat by beat constant DI equal to 400 msec for 200 beats with different values of I_{CaL}. It was noted that a difference in nominal I_{CaL} of 1.95 pA/pF was observed between the ascending and descending phases at the 400 msec mean DI (as shown in figure 11 and table 2, points G and H). Therefore, we altered the levels of L-type calcium channel current for the constant DI control protocol. It was determined that a 5% increase and a 3% decrease in I_{CaL} resulted in integrated currents of -43.57 pA/pF and -41.63 pA/pF, respectively, thus giving a difference of 1.95 pA/pF. The thickness of the hysteresis loop during the simulated 400 msec sinusoidal protocol at

nominal I_{CaL} was 10 msec. Yet, during the constant DI pacing, the steady state APDs changed from 206 msec (at a 5% increase in I_{CaL}) to 202 msec (at a 3% decrease in I_{CaL}), giving a difference in APD of 4 msec. However, during the ascending phase (which corresponds to the lower half of the hysteresis loop) integrated I_{CaL} was larger but the sodium/calcium exchanger current was smaller than that during the descending phase. Since calcium is a divalent ion, movement of a Ca^{2+} ion through the L-type calcium channel brings in a net positive charge of two, while the sodium/calcium exchanger only brings in a net positive charge of one. However, during the ascending phase, the APDs were shorter by about 10 msec than the descending phase. These results suggest that unlike previous simulations using the Luo-Rudy dynamic model [18], in the CVM model, the effect of a change in Ca_i on the sodium/calcium exchanger current influenced membrane potential, and therefore APDs, more than the effect on I_{CaL} did.

Manipulation of free intracellular calcium:

Results from the BAPTA-AM study were statistically not significant between pre and post manipulation. Yet, BAPTA-AM has been used previously, by Walker et al., in studies of alternans hysteresis and results were shown to be conclusive. The hysteresis in that study is different from our study as their hysteresis is defined as memory in alternans, i.e. the threshold at which alternans begin and end, as well as the difference in amplitudes of alternans as the pacing rate increases and decreases in a sequential oscillatory pattern [20].

There are six possible explanations as to why significant results were not found: failure to load due to superfusing, temperature, dosage, light, sample size and no effect on memory. As discussed previously, the Walker study had found statistically significant results, whereas we did not. Since they used the same amount of BAPTA-AM as we did (0.5 μM/L) there are only two notable differences: the difference in perfusion and superfusion, and temperature. The most probable explanation for the results that we found is that BAPTA-AM did not load into the cells from where we recorded. As seen in the methods section, our setup was one with superfusion, i.e. where the solution runs over the surface of the tissue. Since myocytes are tightly packed, with little space in between

each cell, molecules with a very small size, like oxygen, pass easily in between cells in the top layer. However, large molecules, like BAPTA-AM may not be able pass with the same degree of mobility between the first layer of myocytes to load into cells much below the top layer. This could explain why we had live cells to record from, and good TMPs, but no statistically significant results. Perhaps, if we had perfused the heart, where it is thought that there is at least one capillary to deliver molecules for each myocyte [45], BAPTA-AM might have loaded into all the myocytes, producing a significant effect on memory. The other noted difference between our study and Walker's is the temperature at which the studies were carried out. Walker et al. conducted their study at around room temperature (~22ºC) whereas our experiment was done around physiological temperature (~37ºC) [20]. Room temperature may be a better facilitator of BAPTA-AM loading than physiological temperature. If this is the case, in future studies, either the temperature needs to be lowered to room temperature during loading, or a larger amount of BAPTA-AM should be used at physiological temperature, as there have been conclusive BAPTA-AM studies carried out at 37ºC with higher BAPTA-AM levels [28]. However, this seems unlikely to be a problem as diffusion is proportionally related to temperature, therefore higher loading temperatures should have facilitated the loading of BAPTA-AM.

The other less likely explanations are explained as follows. The MSDS sheets for BAPTA-AM do state that it is sensitive to light and as such, great measures were taken to avoid light exposure; BAPTA-AM was stored in a light resistant bottle, and during loading, ambient light was lessened as much as possible. Yet, there was some light exposure during the mixing process of BAPTA-AM in DMSO, possibly a minute amount of exposure during loading and, finally, the experiments were carried out in a well lit room. Although, it is unlikely that light exposure was the reason for the insignificant findings of the experiment as no other studies reported working under stringent lighting conditions. Another alternative explanation may be that the sample size of the study was too small to determine statistical significance, however this is also unlikely as this sample size was more than adequate for the verapamil study as well as the Walker study [20]. Finally, one last hypothesis is simply that BAPTA-AM does not have an effect on

memory and hysteresis. Therefore, in light of these hypotheses, a concrete explanation cannot be given without further study, with first priorities going to perfusion/superfusion during loading, temperature during loading, and the amount of BAPTA-AM used.

In summary, our studies show that a decrease in I_{CaL} decreases the measures of memory defined by the parameters area, thickness, overall tilt, max delay and min delay, whereas the chelation of Ca_i studies were inconclusive on hysteresis in restitution of APD during sequential and oscillatory changes in DI. This decrease in memory, seen through the use of verapamil, taken together with the decrease in slope of restitution of APD with a decrease in I_{CaL} previously reported by others [22, 35, 36], suggests that the effect of decrease in I_{CaL} on stability of activation may be more complicated than what is suggested by the use of slope of restitution alone, especially if memory does indeed increase stability as predicted by theory [6, 17, 34]. As stated previously, these results also show that use of sequential changes in DI can reveal additional features of APD dynamics, unlike what which is seen with the contemporary protocols.

Chapter Six: Limitations

The results from this study were obtained from the endocardial side of right ventricular tissue in pigs. Given the heterogeneity that is known to exist among species and within different regions of the heart, it is not known whether or not these results will apply to other regions of the heart, or to other mammalian species, especially humans. The simulation results suggest a possible explanation of the observed changes due to reduced I_{CaL}. However, it is recognized that the choice of our model (which is for a canine ventricular myocyte) is a limitation as our experiments were carried out on pigs. It should be noted, however, that we had no alternate models that could have removed this limitation as no ionically detailed model exists of pig ventricular myocytes. Also, the limitations inherent in these models is recognized, as not all experimental changes in hysteresis parameters could be simulated by a single level of change in I_{CaL}.

In addition we note that the BAPTA-AM studies were found to be inconclusive and need to be carried out again with more rigorous guidelines when it comes to perfusion, temperature, sample size and perhaps a higher dosage of drug administration.

References

1. American Heart Association, I. *Sudden Cardiac Death*. 2009; Available from: http://www.americanheart.org/presenter.jhtml?identifier=4741.

2. Walker, M.L. and D.S. Rosenbaum, *Repolarization alternans: implications for the mechanism and prevention of sudden cardiac death.* Cardiovasc Res, 2003. **57**(3): p. 599-614.

3. Yue, D.T., et al., *Postextrasystolic potentiation of the isolated canine left ventricle. Relationship to mechanical restitution.* Circ Res, 1985. **56**(3): p. 340-50.

4. Elharrar, V. and B. Surawicz, *Cycle length effect on restitution of action potential duration in dog cardiac fibers.* Am J Physiol, 1983. **244**(6): p. H782-92.

5. Nolasco, J.B. and R.W. Dahlen, *A graphic method for the study of alternation in cardiac action potentials.* J Appl Physiol, 1968. **25**(2): p. 191-6.

6. Cherry, E.M. and F.H. Fenton, *Suppression of alternans and conduction blocks despite steep APD restitution: electrotonic, memory, and conduction velocity restitution effects.* Am J Physiol Heart Circ Physiol, 2004. **286**(6): p. H2332-41.

7. Weiss, J.N., et al., *Chaos and the transition to ventricular fibrillation: a new approach to antiarrhythmic drug evaluation.* Circulation, 1999. **99**(21): p. 2819-26.

8. Karma, A., *Electrical alternans and spiral wave breakup in cardiac tissue.* Chaos, 1994. **4**(3): p. 461-472.

9. Koller, M.L., M.L. Riccio, and R.F. Gilmour, Jr., *Dynamic restitution of action potential duration during electrical alternans and ventricular fibrillation.* Am J Physiol, 1998. **275**(5 Pt 2): p. H1635-42.

10. Qu, Z., et al., *Mechanisms of discordant alternans and induction of reentry in simulated cardiac tissue.* Circulation, 2000. **102**(14): p. 1664-70.

11. Rosenbaum, D.S., et al., *Electrical alternans and vulnerability to ventricular arrhythmias.* N Engl J Med, 1994. **330**(4): p. 235-41.

12. Banville, I., N. Chattipakorn, and R.A. Gray, *Restitution dynamics during pacing and arrhythmias in isolated pig hearts.* J Cardiovasc Electrophysiol, 2004. **15**(4): p. 455-63.

13. Choi, B.R., T. Liu, and G. Salama, *Adaptation of cardiac action potential durations to stimulation history with random diastolic intervals.* J Cardiovasc Electrophysiol, 2004. **15**(10): p. 1188-97.

14. Goldhaber, J.I., et al., *Action potential duration restitution and alternans in rabbit ventricular myocytes: the key role of intracellular calcium cycling.* Circ Res, 2005. **96**(4): p. 459-66.

15. Jordan, P.N. and D.J. Christini, *Determining the effects of memory and action potential duration alternans on cardiac restitution using a constant-memory restitution protocol.* Physiol Meas, 2004. **25**(4): p. 1013-24.

16. Saitoh, H., J.C. Bailey, and B. Surawicz, *Alternans of action potential duration after abrupt shortening of cycle length: differences between dog Purkinje and ventricular muscle fibers.* Circ Res, 1988. **62**(5): p. 1027-40.

17.	Wu, R. and A. Patwardhan, *Restitution of action potential duration during sequential changes in diastolic intervals shows multimodal behavior.* Circ Res, 2004. **94**(5): p. 634-41.

18.	Wu, R. and A. Patwardhan, *Effects of rapid and slow potassium repolarization currents and calcium dynamics on hysteresis in restitution of action potential duration.* J Electrocardiol, 2007. **40**(2): p. 188-99.

19.	Lorente, P., et al., *Analytical modeling of the hysteresis phenomenon in guinea pig ventricular myocytes.* Acta Biotheor, 1992. **40**(2-3): p. 177-93.

20.	Walker, M.L., et al., *Hysteresis effect implicates calcium cycling as a mechanism of repolarization alternans.* Circulation, 2003. **108**(21): p. 2704-9.

21.	Fox, J.J., J.L. McHarg, and R.F. Gilmour, Jr., *Ionic mechanism of electrical alternans.* Am J Physiol Heart Circ Physiol, 2002. **282**(2): p. H516-30.

22.	Tolkacheva, E.G., J.M. Anumonwo, and J. Jalife, *Action potential duration restitution portraits of mammalian ventricular myocytes: role of calcium current.* Biophys J, 2006. **91**(7): p. 2735-45.

23.	Levick, J.R., *An introduction to cardiovascular physiology*. 4 ed. 2003: Arnold, a member of the Hodder Headline Group.

24.	*Acute Myocardial Infarction*. Available from: rezidentiat.3x.ro/eng/tulbritmeng.htm.

25.	Online, D.I. *Verapamil Official FDA information, side effects and uses*. 09/2008; Available from: http://www.drugs.com/pro/verapamil.html.

26.	Guimarães, C.R.W., et al., *On the application of simple explicit water models to the simulations of biomolecules* Braz. J. Phys, 2004. **34**.

27.	Sun, Y., C. Caputo, and K.A. Edman, *Effects of BAPTA on force and Ca2+ transient during isometric contraction of frog muscle fibers.* Am J Physiol, 1998. **275**(2 Pt 1): p. C375-81.

28.	Leitch, S.P. and H.F. Brown, *Effect of raised extracellular calcium on characteristics of the guinea-pig ventricular action potential.* J Mol Cell Cardiol, 1996. **28**(3): p. 541-51.

29.	Winslow, R.L., et al., *Mechanisms of altered excitation-contraction coupling in canine tachycardia-induced heart failure, II: model studies.* Circ Res, 1999. **84**(5): p. 571-86.

30.	Goldberger, A.L. and B.J. West, *Fractals in physiology and medicine.* Yale J Biol Med, 1987. **60**(5): p. 421-35.

31.	Garfinkel, A., et al., *Preventing ventricular fibrillation by flattening cardiac restitution.* Proc Natl Acad Sci U S A, 2000. **97**(11): p. 6061-6.

32.	Huang, J., et al., *Restitution properties during ventricular fibrillation in the in situ swine heart.* Circulation, 2004. **110**(20): p. 3161-7.

33.	Wu, T.J., et al., *Two types of ventricular fibrillation in isolated rabbit hearts: importance of excitability and action potential duration restitution.* Circulation, 2002. **106**(14): p. 1859-66.

34.	Chialvo, D.R., D.C. Michaels, and J. Jalife, *Supernormal excitability as a mechanism of chaotic dynamics of activation in cardiac Purkinje fibers.* Circ Res, 1990. **66**(2): p. 525-45.

35.	Mahajan, A., et al., *Modifying L-type calcium current kinetics: consequences for cardiac excitation and arrhythmia dynamics.* Biophys J, 2008. **94**(2): p. 411-23.

36.   Riccio, M.L., M.L. Koller, and R.F. Gilmour, Jr., *Electrical restitution and spatiotemporal organization during ventricular fibrillation.* Circ Res, 1999. **84**(8): p. 955-63.

37.   Amitzur, G., et al., *Modulation of ventricular fibrillation in the isolated heart: the role of slow calcium channel activity under continuous perfusion.* J Cardiovasc Pharmacol, 2000. **35**(1): p. 16-28.

38.   Boriani, G., et al., *A controlled study on the effect of verapamil on atrial tachycaarrhythmias in patients with brady-tachy syndrome implanted with a DDDR pacemaker.* Int J Cardiol, 2005. **104**(1): p. 73-6.

39.   Cohen, A.S., M.S. Matharu, and P.J. Goadsby, *Electrocardiographic abnormalities in patients with cluster headache on verapamil therapy.* Neurology, 2007. **69**(7): p. 668-75.

40.   Kalb, S.S., et al., *The restitution portrait: a new method for investigating rate-dependent restitution.* J Cardiovasc Electrophysiol, 2004. **15**(6): p. 698-709.

41.   Kalb, S.S., et al., *Restitution in mapping models with an arbitrary amount of memory.* Chaos, 2005. **15**(2): p. 23701.

42.   Nielsen, T.D., et al., *Epicardial mapping of ventricular fibrillation over the posterior descending artery and left posterior papillary muscle of the swine heart.* J Interv Card Electrophysiol, 2009. **24**(1): p. 11-7.

43.   Sato, D., et al., *Spatially discordant alternans in cardiac tissue: role of calcium cycling.* Circ Res, 2006. **99**(5): p. 520-7.

44.   Shiferaw, Y., et al., *Nonlinear dynamics of paced cardiac cells.* Ann N Y Acad Sci, 2006. **1080**: p. 376-94.

45.   Van Kerckhoven, R., et al., *Pharmacological therapy can increase capillary density in post-infarction remodeled rat hearts.* Cardiovasc Res, 2004. **61**(3): p. 620-9.

VITA

KATHLEEN GUZMAN

Date of Birth: August 13, 1984
in
Covington, KY

Degree Awarded
Bachelors of Science in Electrical Engineering

University of Kentucky, August 2007